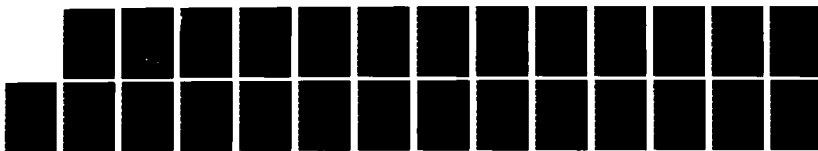


AD-A136 030 ANOMALOUS TRANSPORT IN CURRENT SHEETS(U) NAVAL RESEARCH 1/1
LAB WASHINGTON DC J D HUBA 25 NOV 83 VRL-MR-5220

UNCLASSIFIED

F/G 12/1 NL

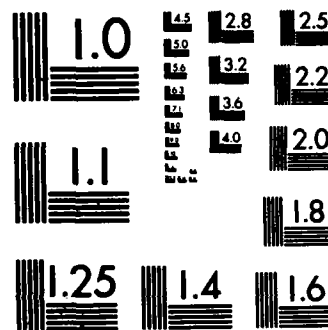


END

FILMED

100

000



MICROCOPY RESOLUTION TEST CHART
NATIONAL BUREAU OF STANDARDS-1963-A

(2)

NRL Memorandum Report 5220

Anomalous Transport in Current Sheets

J. D. HUBA

*Geophysical and Plasma Dynamics Branch
Plasma Physics Division*

November 25, 1983

AD-A236030

DTIC FILE COPY

This research was supported by the National Aeronautics and Space Administration
and the Office of Naval Research.



NAVAL RESEARCH LABORATORY
Washington, D.C.

DTIC
SELECTED
DEC 19 1983
S E D
E

Approved for public release; distribution unlimited.

83 12 16 135

REPORT DOCUMENTATION PAGE		READ INSTRUCTIONS BEFORE COMPLETING FORM
1. REPORT NUMBER NRL Memorandum Report 5220	2. GOVT ACCESSION NO.	3. RECIPIENT'S CATALOG NUMBER
4. TITLE (and Subtitle) ANOMALOUS TRANSPORT IN CURRENT SHEETS		5. TYPE OF REPORT & PERIOD COVERED Interim report on a continuing NRL problem.
7. AUTHOR(s) J.D. Huba		6. PERFORMING ORG. REPORT NUMBER
9. PERFORMING ORGANIZATION NAME AND ADDRESS Naval Research Laboratory Washington, DC 20375		10. PROGRAM ELEMENT, PROJECT, TASK AREA & WORK UNIT NUMBERS W-15494; 61153N; RR033-02-44; 47-1982-0-3; 47-0884-0-3
11. CONTROLLING OFFICE NAME AND ADDRESS National Aeronautics and Space Admin. Office of Naval Research Washington, DC 20546		12. REPORT DATE November 25, 1983
14. MONITORING AGENCY NAME & ADDRESS (if different from Controlling Office)		13. NUMBER OF PAGES 26
		15. SECURITY CLASS. (of this report) UNCLASSIFIED
		15a. DECLASSIFICATION/DOWNGRADING SCHEDULE
16. DISTRIBUTION STATEMENT (of this Report) Approved for public release; distribution unlimited.		
17. DISTRIBUTION STATEMENT (of the abstract entered in Block 20, if different from Report)		
18. SUPPLEMENTARY NOTES This research was supported by the National Aeronautics and Space Administration and the Office of Naval Research.		
19. KEY WORDS (Continue on reverse side if necessary and identify by block number) Anomalous transport Microinstability theory Magnetic reconnection Magnetospheric plasmas		
20. ABSTRACT (Continue on reverse side if necessary and identify by block number) A review of several microinstabilities that have been suggested as possible anomalous transport mechanisms in current sheets is presented. The specific application is to a field reversed plasma which is relevant to the so-called "diffusion region" of a reconnection process. The linear and nonlinear properties of the modes are discussed, and each mode is assessed as to its importance in reconnection processes based upon these properties. It is concluded that the two most relevant instabilities are the ion acoustic instability and the lower-hybrid-drift instability. However, each instability has limitations as far as reconnection is concerned, and more research is needed in this area.		

CONTENTS

I.	INTRODUCTION.....	1
II.	PLASMA AND FIELD CONFIGURATION.....	4
III.	REVIEW OF MICROINSTABILITIES.....	7
	A. Unmagnetized Instabilities.....	7
	1. Buneman instability.....	7
	2. Ion acoustic instability.....	7
	B. Magnetized Instabilities.....	8
	1. Beam cyclotron instability.....	8
	2. Magnetized ion-ion instability.....	8
	3. Lower-hybrid-drift instability.....	9
IV.	APPLICATION TO RECONNECTION.....	9
	A. Unmagnetized Regime ($ x < x_e$)	10
	1. Buneman instability.....	10
	2. Ion acoustic instability.....	10
	B. Magnetized Regime ($ x > x_e$)	10
	1. Beam cyclotron instability.....	10
	2. Magnetized ion-ion instability.....	11
	3. Lower-hybrid-drift instability.....	11
V.	CONCLUDING REMARKS.....	15
ACKNOWLEDGMENTS.....		16
REFERENCES		17

Accession For	
NTIS GRA&I <input checked="" type="checkbox"/>	
DTIC TAB <input type="checkbox"/>	
Unannounced <input type="checkbox"/>	
Justification _____	
By _____	
Distribution/ _____	
Availability Codes	
Dist	Avail and/or Special
A-1	



ANOMALOUS TRANSPORT IN CURRENT SHEETS

I. INTRODUCTION

The subject of anomalous transport in current sheets is of great interest to space plasma physicists, especially as it can impact collisionless reconnection processes. A simple concept of a reconnection process is illustrated in Fig. 1, which depicts a field-reversed plasma. The magnetic field B is in opposite directions on the two sides of the neutral line, and a uniform electric field E is directed into the page. The plasma motion in this configuration is roughly described by Ohm's law, which for the present situation may be written $E + U \times B = \eta J$ where U is the plasma velocity, η the resistivity, and J the current density). Away from the neutral line, the resistivity term is usually small, and the plasma obeys $E + U \times B = 0$, which is sometimes called the frozen-in-field condition. Loosely speaking, this means that particles are tied to a particular magnetic-field line. In this region, far from the neutral line, the plasma and the magnetic field are carried towards the neutral line with a velocity $U_{in} \approx E/B$. However, the frozen-in-field condition breaks down in the diffusion region, where the magnetic field becomes very weak. The governing equation is $E = \eta J$, and the plasma and magnetic field are decoupled, i.e., no longer tied together. When this occurs the magnetic field can slip through the plasma and reconnect. The plasma and magnetic field then leave the diffusion region with a velocity U_{out} as shown in Fig. 1. In this process $U_{out} > U_{in}$, so that the plasma energy has been increased at the expense of magnetic-field energy.

One of the problems in applying this model to collisionless space plasmas (such as the earth's magnetotail) is properly describing the diffusion region. The resistivity η associated with coulomb collisions between particles is very small in space; the plasma is essentially collisionless. What then can balance the electric field in the diffusion region? There are other terms in Ohm's law, such as electron inertia and pressure anisotropy, but these also appear to be quite small (Vasiliunas, 1975). Another explanation is the occurrence of anomalous resistivity in the diffusion region. In this situation, particles scatter off collective electric fields generated by a plasma microinstability, and this scattering

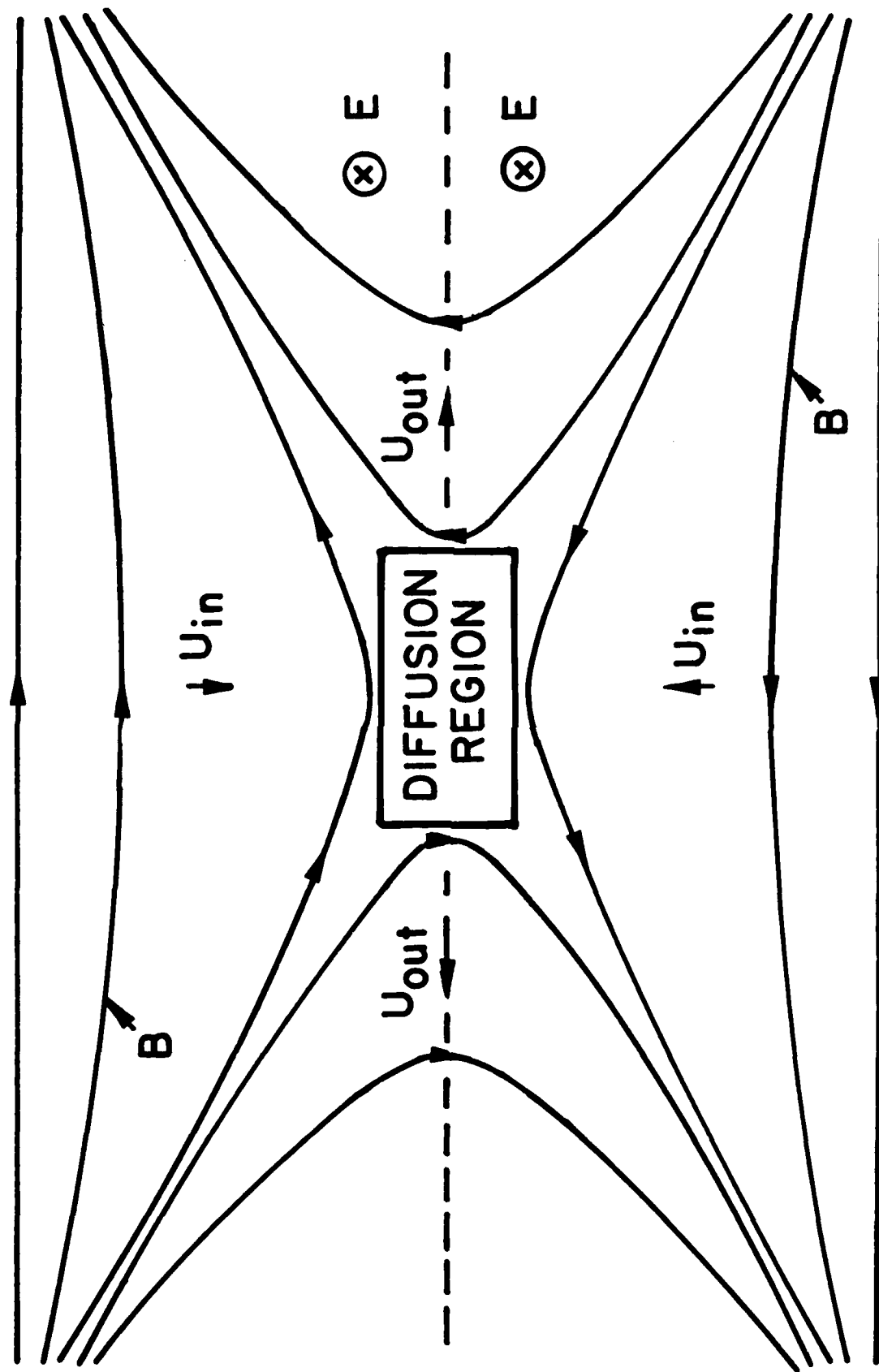


Figure 1: Schematic of a forced reconnection process.

process decouples the plasma from the magnetic field. Recent laboratory experiments (Gekelman et al., 1982; Stenzel et al., 1983) in fact report observations of anomalous scattering.

Incorporating microturbulence effects in a reconnection process is a formidable task. Several issues need to be addressed. First, the linear theory of a microinstability needs to be developed appropriate for the plasma and magnetic field configuration of the diffusion region. In this study it is important to determine the relevant plasma conditions needed to excite the instability (e.g., width of the current sheet, electron/ion temperature ratio, etc.). Second, a nonlinear theory of the microinstability in question needs to be developed. Here, it is crucial to determine the level of microturbulence produced by the instability (i.e., saturation energy), and whether or not the turbulence is steady state. Finally, given the linear and nonlinear properties of the unstable waves, this information needs to be self-consistently incorporated into the hydrodynamic flows associated with a reconnection process. Development of such a self-consistent theory of collisionless reconnection is indeed difficult.

In general, plasma theorists have focussed on the first two issues: the linear and nonlinear theories of a microinstability as it applies to the diffusion region. The final issue, incorporating turbulence into reconnection flows, has been ignored. [A notable exception to this is the work of Coroniti and Eviatar (1977).] Although this may be considered, perhaps, a "cop-out" on the part of plasma theorists, the information regarding plasma microturbulence in the diffusion region is still crucial to understanding the overall process. Moreover, the anomalous transport properties of instabilities in the diffusion region can be modelled and incorporated into 2D and 3D MHD simulations of reconnection (Sato and Hayashi, 1980; Ugai, 1983; Sato, these proceedings). Although this is not self-consistent, it does provide insight into the collisionless reconnection process.

In this spirit, the purpose of this paper is to review the various microinstabilities that have been suggested to play a role in reconnection phenomena. Hence, only the linear and nonlinear properties of the instabilities will be discussed. Based upon these properties one can then

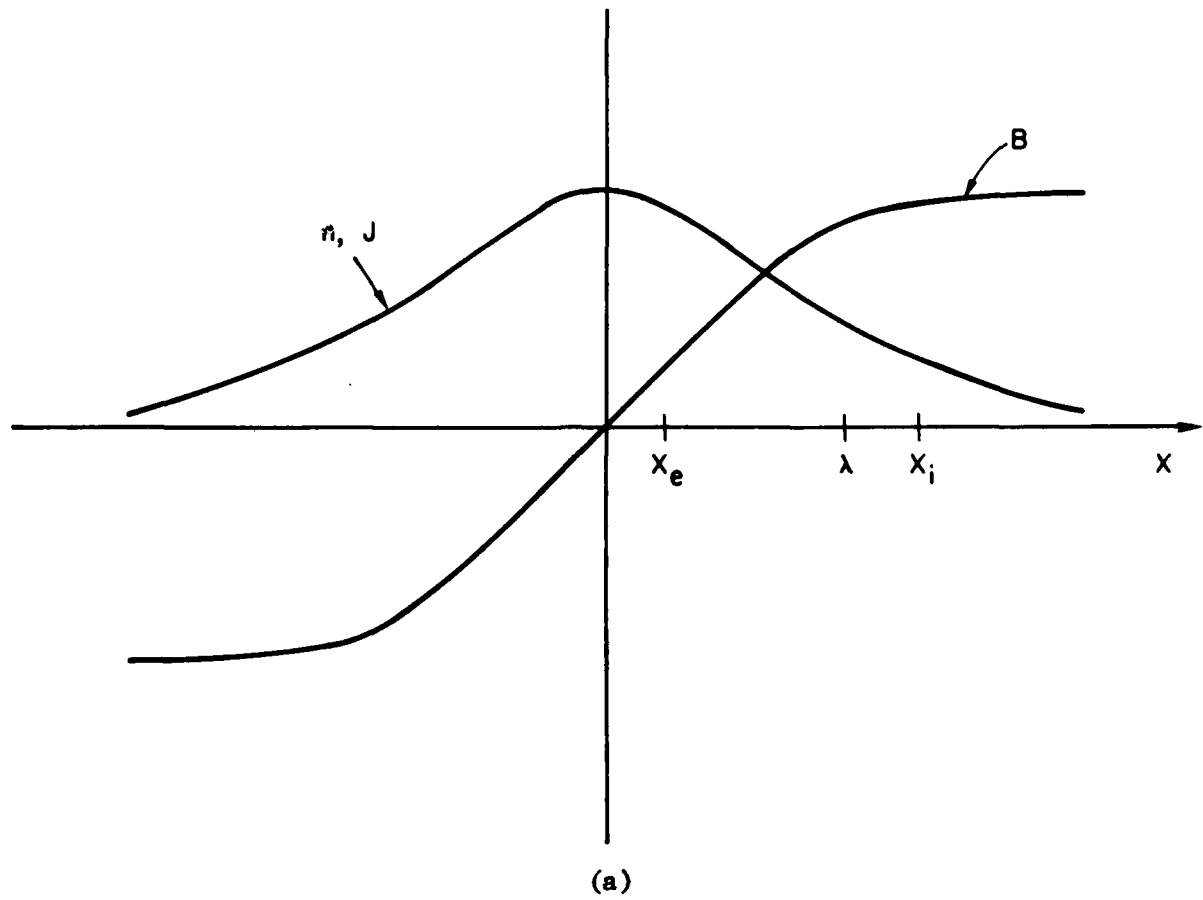
assess whether or not a particular instability is a viable source of anomalous resistivity for a reconnection process. Finally, it should be noted that a review article of this nature has been published (Papadopoulos, 1979). The present work, in fact, draws heavily from Papadopoulos (1979); however, we attempt to elucidate certain aspects of the problem not emphasized in Papadopoulos (1979), and to present new results that have been obtained in the past four years.

The organization of the paper is as follows. In the next section, we describe the basic plasma and magnetic field configuration under consideration. In Section III, a description of the linear and nonlinear properties of several macroinstabilities is given. In Section IV, a discussion of the relevance of each of these instabilities to a reconnection process is presented. Finally, the last section contains a summary of the important results obtained to date.

II. PLASMA AND FIELD CONFIGURATION

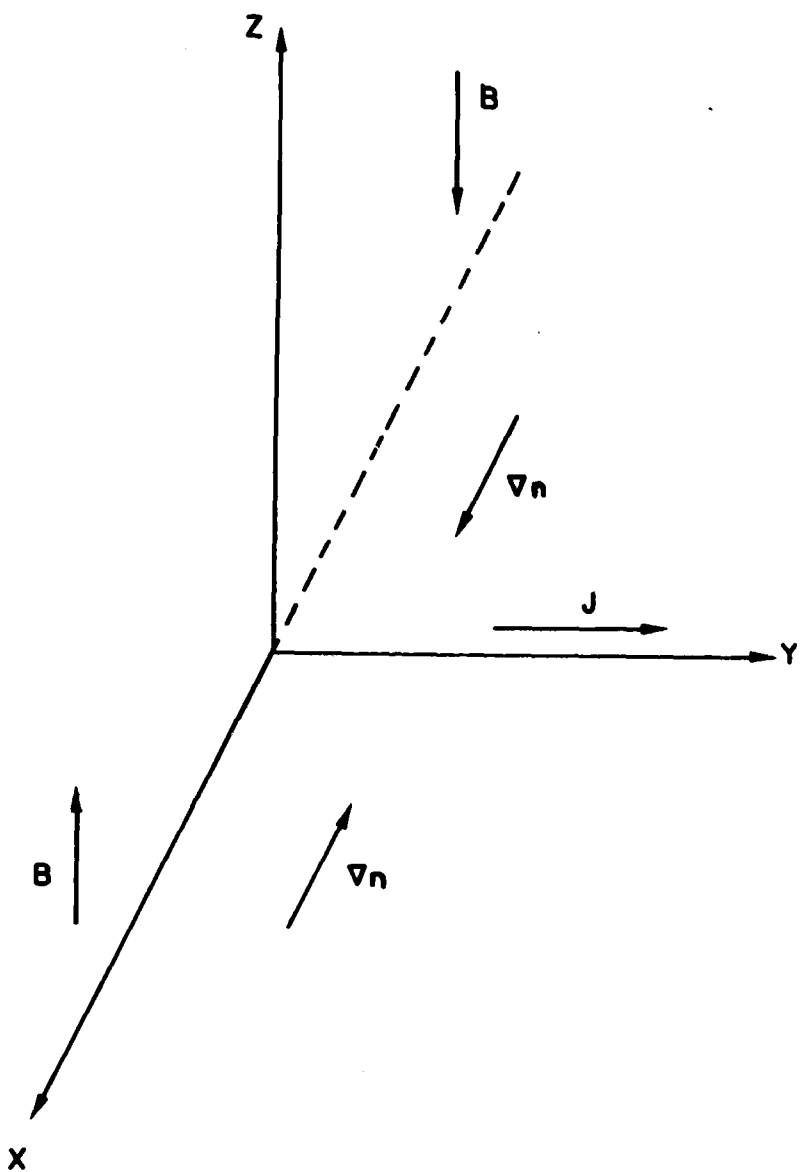
The basic plasma and magnetic field configuration to be considered in this review is shown in Fig. 2. We take a simple, 1D reversed field geometry shown in Fig. 2a. The magnetic field B reverses direction at $x = 0$ and is supported by a plasma current J which is peaked at $x = 0$. The width of the reversal layer (or current sheet) is given by λ . An important parameter shown in Fig. 2a is x_e and x_i where $x_\alpha = (2\rho_\alpha\lambda)^{1/2}$, where ρ_α is the mean Larmor radius of the α species, and typically $x_e \ll \lambda \ll x_i$. This parameter will be discussed shortly. In Fig. 2b, the slab geometry used in the stability analysis is shown. The magnetic field B is in the + or - z direction, the density gradient ∇n is directed towards $x = 0$, the magnetic field gradient ∇B is directed away from $x = 0$, and the current J is in the y direction. For the purposes of this review, the microinstabilities discussed are driven solely by the cross-field current J . Thus, the wave vector k for the instabilities discussed is in the same direction as J , i.e., $k = k \hat{e}_y$. Instabilities driven by particle distribution functions which include beams, tails, or temperature anisotropies are not considered.

Finally, we make one further simplifying assumption in the analysis which concerns the parameter $x_\alpha = (2\rho_\alpha\lambda)^{1/2}$ (Hoh, 1966). This quantity



(a)

Figure 2: Plasma configuration and geometry.



(b)

Figure 2 (Cont'd): Plasma configuration and geometry.

indicates the boundary of crossing and non-crossing thermal particles. Thermal particles in the region $|x| < x_a$ cross the "neutral line", i.e., pass through the magnetic null region $B = 0$ at $x = 0$. These particles execute rather complicated orbits not amenable to analysis. On the other hand, thermal particles in the region $|x| > x_a$ do not cross the "neutral line". These particles are magnetized and execute gyro-orbits about \vec{B} . Thus, we consider two regimes: unmagnetized electrons ($|x| < x_e$) and magnetized electrons ($|x| > x_e$). The ions are taken to be unmagnetized which is valid for $|x| < x_i$ or $\gamma > \Omega_i$ where γ is the growth rate of an instability and $\Omega_i = eB/m_i c$ is the ion gyrofrequency. The assumption of unmagnetized electrons (i.e., "straight line orbits") is an oversimplification but is reasonably valid for $|x| \ll x_e$.

III. REVIEW OF MICROINSTABILITIES

A. Unmagnetized Instabilities

1. Buneman instability

The Buneman instability is the classic electron-ion two-stream instability (Buneman, 1959). It is a fluid-like (or hydrodynamic) instability in that it does not involve wave-particle resonances (i.e., $\omega/k \gg v_a$ where $v_a = (T_a/m_a)^{1/2}$ is the thermal velocity of species a). The turn-on condition for instability is roughly $V_d \gtrsim 2v_e$ where V_d is the relative electron-ion drift. In the linear regime at maximum growth one finds that $\omega_r = \omega_{pe}$, $\gamma \approx (m_e/m_i)^{1/3} \omega_{pe}$ and $k \approx V_d / \omega_{pe} \lesssim \lambda_{de}^{-1}$ where $\omega = \omega_r + i\gamma$, $\omega_{pe} = (4\pi n_e^2 / m_e)^{1/2}$ is the electron plasma frequency, and $\lambda_{de} = v_e/\omega_{pe}$ is the electron Debye length (Krall and Trivelpiece, 1973). Thus, the instability is considered to be high frequency and short wavelength. In the nonlinear regime the instability is saturated by electron trapping which leads to strong electron heating (i.e., $v_e \gtrsim V_d$) (Davidson et al., 1970; Biskamp and Chodura, 1973). In the presence of a steady state electric field, the anomalous resistivity η_{an} is not steady state (i.e., $\eta_{an} \sim \text{constant}$) but is spiky (Papadopoulos, 1977).

2. Ion-acoustic instability

The ion-acoustic instability, like the Buneman instability, is driven by the relative electron-ion drift V_d . However, the ion acoustic instability is a resonant (or kinetic) instability and is driven via an electron-wave resonance. The turn-on condition for this instability is

somewhat less stringent than that of the Buneman instability when $T_e \gg T_i$. The condition is approximately $V_d \gtrsim (T_i/m_e)^{1/2}$ for $0.2 < T_e/T_i < 5.0$ (Coroniti and Eviatar, 1977). However, when $T_e \lesssim T_i$ the turn-on is comparable to that of the Buneman instability. Linear theory predicts (at maximum growth) that $\omega_r \approx kc_s \approx \omega_{pi}$, $\gamma \approx (m_e/m_i)^{1/2} (V_d/c_s)\omega_{pe}$ and $(4\pi ne^2/m_i)^{1/2} k \sim \lambda_d^{-1}$ where $c_s = (T_e/m_i)^{1/2}$ is the ion sound speed and $\omega_{pi} = (4\pi ne^2/m_i)^{1/2}$ is the ion plasma frequency (Papadopoulos, 1979).

There have been many nonlinear theories of the ion-acoustic instability proposed (e.g., quasilinear, resonance broadening, nonlinear Landau damping). Rather than discuss any of these theories in detail I will simply be noted that (1) a steady state anomalous resistivity can be achieved (Coroniti and Eviatar, 1977), and (2) near marginal stability, the anomalous collision frequency is roughly $\nu_{an} \approx 10^{-2}\omega_{pe}$ (Papadopoulos 1979) so that the anomalous resistivity is $\eta_{an} = 4\pi\nu_{an}/\omega_{pe}^2 \approx 10^{-1}\omega_{pe}^{-1}$.

B. Magnetized Instabilities

1. Beam cyclotron instability

The beam cyclotron instability (also known as the electron cyclotron drift instability) (Wong, 1970; Lampe et al., 1972) is a fluid-like (or hydrodynamic) instability that is excited via the coupling of an electron Bernstein wave to an ion mode. The relative electron-ion drift allows the ion mode to be Doppler-shifted so that its frequency matches an electron cyclotron harmonic. The turn-on condition for this instability is $V_d > \text{Max} [c_s, (\Omega_e/\omega_{pe})v_e]$ where $c_s = (T_e/m_i)^{1/2}$ (Papadopoulos, 1979). For the case $T_e \ll T_i$, maximum growth is characterized by $\omega_r \approx k(c_s + V_d)$, $\gamma \approx (m_e/m_i)^{1/4}\Omega_e$ and $k \approx \lambda_{de}^{-1}$ (Lampe et al., 1972). The mode saturates because of turbulent scattering of the electrons which effectively "demagnetize" them and they are unable to maintain coherent gyro-orbits (Lampe et al., 1971). The saturation energy of the instability is relatively small so that a small anomalous collision frequency results:

$$\nu_{an} \approx (V_d/v_e)^3\Omega_e \quad (\text{Papadopoulos, 1979}).$$

2. Magnetized ion-ion instability

The magnetized ion-ion instability (Papadopoulos et al., 1971) is a counter-streaming ion-ion instability. It is a fluid-like (or hydrodynamic) instability. The turn-on condition for this instability is $V_{ii} \gtrsim 2v_i$ where V_{ii} is the relative ion-ion drift. At maximum growth one can show that $\omega_r \approx 0$, $\gamma = \omega_{lh}$ and $k \approx \omega_{lh}/V_{ii}$ where $\omega_{lh} \approx \omega_{pi}/(1 + \omega_{pe}^2/\Omega_e^2)^{1/2}$

is the lower-hybrid frequency. However, the instability is linearly stable when $v_{ii} > v_A(1 + \beta_e)^{1/2}$ where $v_A = B/(4\pi nm_i)^{1/2}$ is the Alfvén velocity and $\beta_e = 8\pi n T_e / B^2$. The mode saturates because of ion trapping and produces strong ion heating as well as a reduction in the relative ion-ion drift velocity. The anomalous ion-ion collision frequency associated with this instability is $\nu_{an} \lesssim 10^{-1} \omega_{lh}$ (Lampe et al., 1975).

3. Lower-hybrid-drift instability

The lower-hybrid-drift instability (Davidson et al., 1977) is a resonant (or kinetic) instability which is excited via an ion-drift wave resonance when $v_{di} \lesssim v_i$ (here, $v_{di} = (v_i^2/\Omega_i) \partial \ln n / \partial x$ is the ion diammagnetic velocity). The turn-on condition for the instability is $v_{di} > v_i(m_e/m_i)^{1/4}$. The instability is characterized at maximum growth by $\omega_r \approx k v_{di} \lesssim \omega_{lh}$, $\gamma \approx (v_{di}/v_i)\omega_r$ and $k\rho_e \sim (T_e/T_i)^{1/2}$ where ρ_e is the mean electron Larmor radius. This instability is relatively insensitive to the temperature ratio T_e/T_i . However, the mode is suppressed in high β plasmas because of an electron VB drift-wave resonance. A variety of nonlinear theories have been suggested for the lower-hybrid-drift instabilities (e.g., quasilinear relaxation, resonance broadening, ion trapping, mode coupling). Again, we will not discuss these in detail but note that the most likely saturation mechanism is mode coupling (Drake et al., 1983). The anomalous collision frequency associated with the turbulence is $\nu_{an} \approx (v_{di}/v_i)^2 \omega_{lh}$ and a steady state resistivity can result from this turbulence.

IV. APPLICATION TO RECONNECTION

Prior to discussing the relevance of each instability discussed in Section III to reconnection, it is important to note a major difference between the magnetized and unmagnetized instabilities. Namely, the spatial region where these instabilities can exist. As noted in Section II the unmagnetized instabilities are limited to $|x| < x_e$, i.e., essentially the null region where $B \approx 0$. This is precisely where one would like microturbulence to exist in order to "decouple" the plasma from the magnetic field. On the other hand, the magnetized instabilities are restricted to $|x| > x_e$, away from the null field region. Thus, these instabilities do not directly produce an anomalous resistivity in the null region. However, the dynamic evolution of the plasma and field in a

reconnection process may allow penetration of the magnetized modes to the region $|x| < x_e$ (e.g., current steepening, convection).

A. Unmagnetized Regime ($|x| < x_e$)

1. Buneman instability

The Buneman instability requires a strong relative electron-ion drift to be excited (i.e., $V_d \gtrsim 2v_e$). By using Ampere's law to relate the width of the current sheet (λ) to the relative drift (V_d), one can show that $\lambda < c/\omega_{pe}$ for this instability to be excited in the diffusion region. Because of the extremely thin current sheet needed, it seems unlikely that the Buneman instability can be of any importance to collisionless reconnection processes.

2. Ion acoustic instability

A theory of reconnection incorporating the ion acoustic instability as a source of anomalous resistivity has been developed by Coroniti and Eviatar (1977). For a detailed discussion, we refer the interested reader to this paper. However, several comments on this work are in order. First, the model developed by Coroniti and Eviatar (1977) is reasonably self-consistent although a number of simplifying assumptions were required for the analysis. Second, they found that steady state reconnection could occur based upon ion acoustic wave turbulence for certain parameter regimes. Third, even though the turn-on condition for the ion acoustic instability is less stringent than that for the Buneman instability, a thin current sheet is still required to excite this mode, i.e., $\lambda \lesssim \text{few } (c/\omega_{pe})$, especially for plasmas such that $T_e \ll T_i$. Finally, although ion acoustic turbulence has been observed in laboratory reconnection experiments (Breitenahl and Yeates, 1970) its exact role is unclear. Moreover, in space plasmas, it is unlikely that current sheets develop as thin as required for this instability (e.g., the earth's magnetotail). Thus, the ion acoustic instability is probably not important for reconnection processes in collisionless space plasmas.

B. Magnetized Regime ($|x| > x_e$)

1. Beam cyclotron instability

The beam cyclotron instability has been discussed in regard to reconnection by Coroniti and Eviatar (1977) and by Haerendel (1978). As noted by Papadopoulos (1979), thin current sheets ($\lambda \lesssim \text{few } (c/\omega_{pe})$) are needed to produce a significant anomalous resistivity. Also, it has been

shown that a magnetic field gradient (∇B) substantially reduces the growth rate of this instability (Gary, 1972; Sanderson and Priest, 1972). Thus, we conclude that the beam cyclotron instability is not important to reconnection processes.

2. Magnetized ion-ion instability

The magnetized ion-ion instability has recently been proposed as a source of anomalous resistivity for magnetotail reconnection by Lee (1982). However, the plasma configuration required is somewhat more complicated than shown in Fig. 2a. That is, a second electron and ion species is also considered as shown in Fig. 3. This second plasma is labelled untrapped. At the position $x = x_0$ in Fig. 3, the diamagnetic drifts of the two ion species are in opposite directions so that ion counter-streaming occurs. Based on this type of plasma configuration, Lee (1982) finds that the magnetized ion-ion instability can be unstable. It should be noted that (1) the scale lengths of the density gradients need to be relatively sharp ($L_n < \rho_i$ where $L_n \approx (\partial \ln n / \partial x)^{-1}$) in order that the instability turn-on $V_{ii} > 2v_f$; (2) the mode is stable in high β plasmas; and (3) the important effect of electron ∇B damping has been ignored in Lee (1982).

3. Lower-hybrid-drift instability

The lower-hybrid-drift instability was first proposed by Huba et al. (1977) as a source of anomalous resistivity for reconnection in the earth's magnetotail. Two factors in favor of this instability are (1) the mode can be excited in relatively broad current sheets ($\lambda < (m_i/m_e)^{1/4} \rho_i$), and (2) the mode is insensitive to the temperature ratio T_e/T_i . Both of these factors should be contrasted to, say, the requirements for the ion acoustic instability. A subsequent study determined that turbulence observed in the distant magnetotail was consistent with the occurrence of the lower-hybrid-drift instability (Huba et al., 1978). However, a problem with this instability (as it applies to a reconnection process) is that the mode is damped in a high β plasma ($\beta \gg 1$) because of an electron ∇B drift-wave resonance. Thus, based upon both a local and nonlocal linear analysis (Huba et al., 1980), the instability is stable in the near vicinity of the null point.

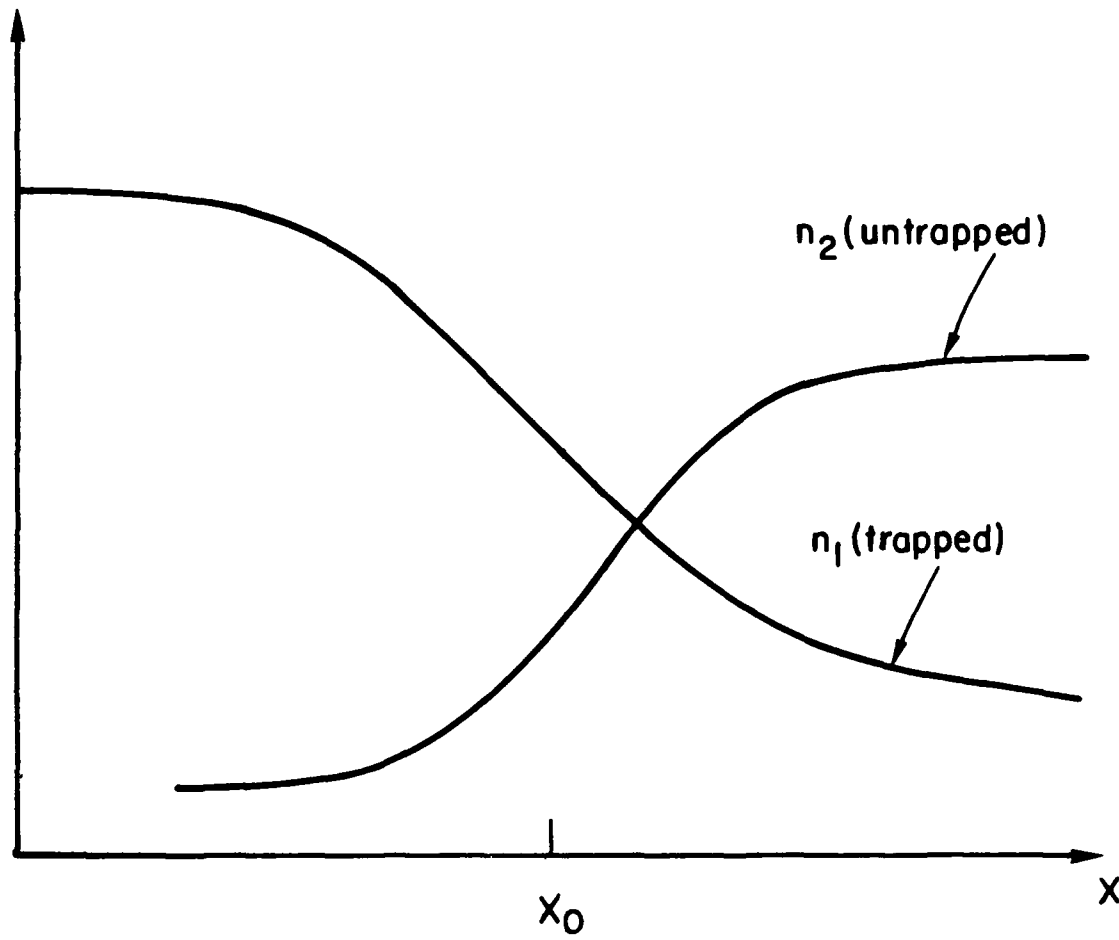


Figure 3: Equilibrium for ion-ion instability.

Although this result is unfavorable in directly providing an anomalous resistivity in the diffusion region, the evolution of the magnetic field in the presence of a resistivity based upon the nonlocal mode structure of the lower-hybrid-drift instability has been investigated (Drake et al., 1981). In this regard, a 1D transport equation for the magnetic field has been developed for an arbitrary resistivity profile in a field-reversed plasma. The equation is given by

$$\frac{\partial B}{\partial t} + \frac{cE}{B} \frac{\partial B}{\partial x} - \frac{2B}{B^2 + B_\ell^2} \frac{\partial}{\partial x} v_{an} \rho_{es}^2 B \frac{\partial B}{\partial x} = \frac{2B}{B^2 + B_\ell^2} \frac{\partial B_\ell}{\partial t} \quad (1)$$

where $B_\ell = B$ (outer boundary) and $\rho_{es}^2 = \rho_e^2 (T_i/T_e)$. On the LHS of Eq. (1) the first term represents the time rate of change of the magnetic field, the second term represents convection because of the inductive electric field E , and the third term represents diffusion based upon an arbitrary collision frequency v_{an} . The RHS side of Eq. (1) contains the effect of a time-varying boundary field.

We have solved Eq. (1) numerically (Drake et al., 1981). A resistivity model such that $\eta \propto B^2$ was chosen; this model has the feature that $\eta = 0$ at the neutral line, but $\eta \neq 0$ away from the neutral line. The results of this work are illustrated in Fig. 4. The initial magnetic field (Fig. 4a) and current density (Fig. 4b) profiles are labeled $\tau = 0$; the profiles at a later time are labeled $\tau = 0.2$. It is found that magnetic flux is transported towards the neutral line and that the current density increases at the neutral line which is due to a diffusion process. This leads to the possibility that waves can subsequently penetrate to the neutral region during the nonlinear evolution of the field-reversed plasma. Such an evolution has been observed in particle simulations of field-reversed plasmas (Winske, 1981; Tanaka and Sato, 1981). However, these simulations used unrealistic mass ratios and it is unclear at this time whether or not wave penetration occurs using realistic mass ratios (Quest, private communication).

Finally, recently a 2D mode coupling nonlinear theory of the lower-hybrid-drift instability has been developed (Drake et al., 1983). This theory is consistent with both laboratory measurements of the instability as well as with computer simulations. An important result from this new

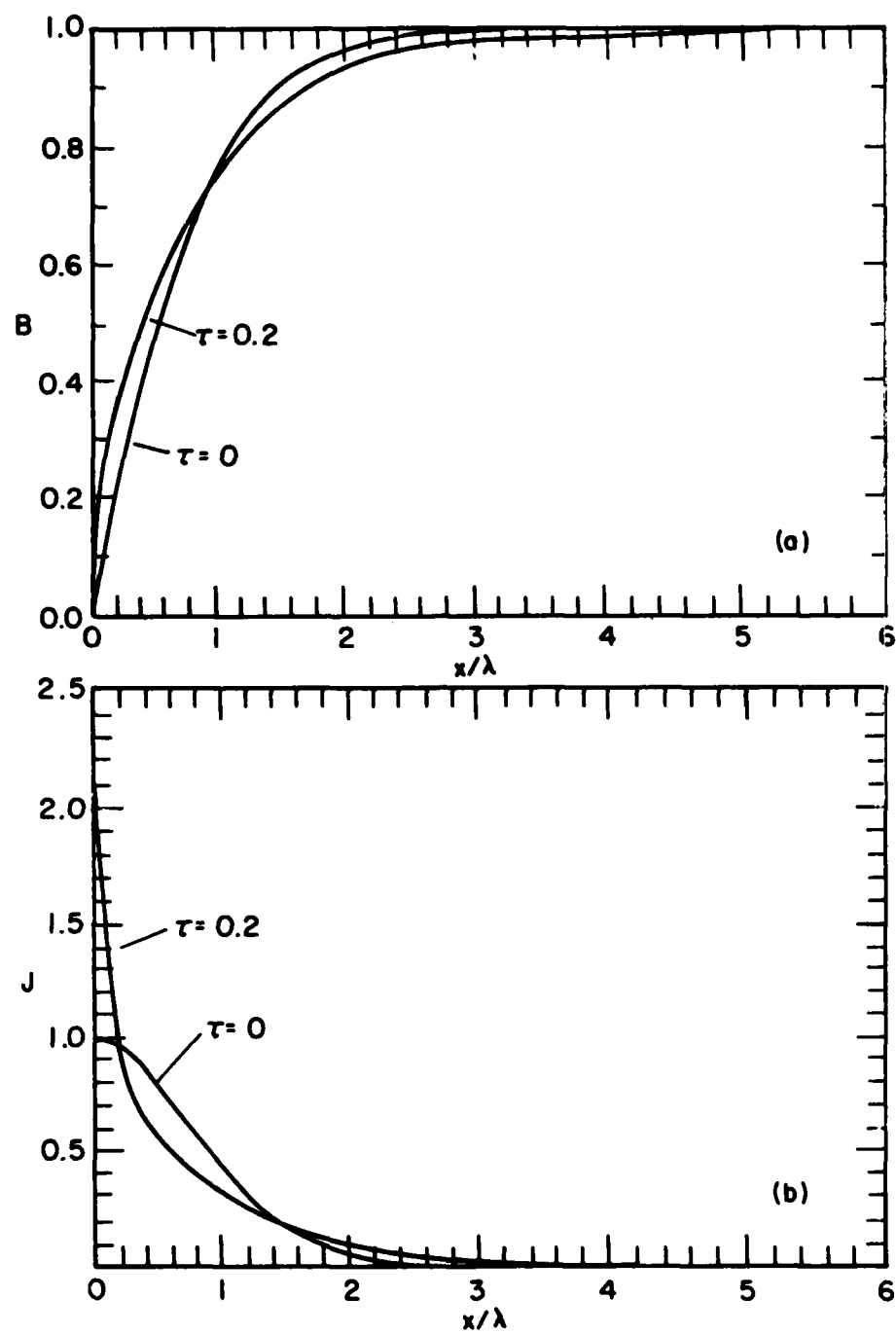


Figure 4: Time evolution of B and J based upon Eq. (1).

theory is an estimate of the anomalous resistivity associated with the turbulence: $v_{an} \approx 2.4(\rho_i/\lambda)^2\omega_{lh}$. This value of v_{an} corresponds to a magnetic Reynolds number of $R_m \approx 0.5 (\rho_i/m_e)^{1/2}(\lambda/\rho_i)^3$. Thus, it is found that the lower-hybrid-drift instability only provides significant anomalous transport for current sheets such that $\lambda \approx \rho_i$. Also, a discussion of this instability as it applies to substorm dynamics is given in Huba et al. (1981).

V. CONCLUDING REMARKS

It is well known that microinstabilities can affect the dynamic evolution of plasmas through wave-particle interactions (i.e., scattering) and cause anomalous diffusion, momentum transfer and energy exchange. The purpose of this review is to briefly discuss several instabilities that have been proposed as anomalous transport mechanisms in current sheets. The focus has been on reversed magnetic field configuration (Fig. 2a), as they relate to collisionless reconnection processes since the presence of microturbulence in the diffusion region can influence the hydrodynamic flows. However, the stability analysis of waves in the diffusion region is difficult and simplifying assumptions are made, as noted in Section II.

The two "favored" instabilities are the ion acoustic instability and lower-hybrid-drift instability. The ion acoustic instability can be excited in the null field region but requires quite thin current sheets ($\lambda \lesssim \text{few } (c/\omega_{pe})$) and is more easily excited in hot electron plasmas ($T_e \gg T_i$). Although it has been observed in laboratory reconnection experiments where these conditions can be met, its occurrence in relevant space plasmas is rather unlikely (e.g., the earth's magnetotail). On the other hand, the lower-hybrid-drift instability has received considerable attention since it can be excited in broader current sheets ($\lambda \sim \rho_i$) and is relatively insensitive to T_e/T_i . However, the waves are strongly damped close to the null region. In a dynamic situation (e.g., forced reconnection), lower-hybrid-drift wave turbulence may penetrate the null region, but this result is tentative at this time. Nonetheless, even if this turbulence does not penetrate the null region, it is likely to exist over a substantial portion of the current sheet and can strongly affect plasma flow in the regions where the mode is unstable. One

possibility is that this instability may limit the width of current sheets to $\lambda \sim \rho_i$ and inertial effects may be dominant in the null region (Coroniti, private communication).

We emphasize that a simplified plasma and field configuration has been used. It is possible that other instabilities may be excited which depend upon non-Maxwellian distribution functions which contain, say, beams and anisotropies. In this regard, laboratory experiments and in situ space observations may indicate more appropriate distribution functions.

Finally, as noted in the introduction, it is crucial to self-consistently incorporate plasma turbulence in the dynamic evolution of collisionless reconnection. This is an exceedingly difficult problem which, perhaps, may only be answered by 3D particle or hybrid simulations, which in themselves are also enormously difficult and beyond present day computational facilities. Maybe our grandchildren will finally solve the problem.

ACKNOWLEDGMENTS

I wish to thank Drs. J. Drake, A. Hassam, F. Coroniti and K. Quest for helpful conversations regarding this problem. This work has been supported by NASA and ONR.

REFERENCES

Biskamp, D., and Chodura, R.: 1973, Phys. Fluids 16, 888.

Bratenahl, A., and Yeates, C.M.: 1970, Phys. Fluids 13, 2696.

Buneman, O.: 1959, Phys. Rev. 115, 503.

Coroniti, F.V., and Eviatar, A.: 1977, Ap. J. Supp. 33, 189.

Davidson, R., Krall, N.A., Papadopoulos, K., and Shanny, R.: 1970, Phys. Rev. Lett. 24, 579.

Davidson, R.C., Gladd, N.T., Wu, C.S., and Huba, J.D.: 1977, Phys. Fluids 20, 301.

Drake, J.F., Gladd, N.T., and Huba, J.D.: 1981, Phys. Fluids 24, 78.

Drake, J.F., Guzdar, P.N., and Huba, J.D.: 1983, Phys. Fluids 26, 601.

Gary, S.P.: 1971, J. Plasma Phys. 6, 561.

Gekelman, W., Stenzel, R.L., and Wild, N.: 1982, J. Geophys. Res. 87, 101.

Haerendel, G.: 1978, J. of Atm. and Terr. Phys. 40, 343.

Hoh, F.C.: 1966, Phys. Fluids 9, 277.

Huba, J.D., Gladd, N.T., and Papadopoulos, K.: 1977 Geophys. Res. Lett. 4, 125.

Huba, J.D., Gladd, N.T., and Papadopoulos, K.: 1978, J. Geophys. Res. 83, 5217.

Huba, J.D., Drake, J.F., and Gladd, N.T.: 1980, Phys. Fluids 23, 552.

Huba, J.D., Gladd, N.T., and Drake, J.F.: 1981, J. Geophys. Res. 86, 5881.

Krall, N.A., and Trivelpiece, A.W.: 1973, "Principles of Plasma Physics", McGraw-Hill Co., NY.

Lampe, M., Manheimer, W.M., McBride, J.B., Orens, J.H., Shanny, R., and Sudan, R.N.: 1971, Phys. Rev. Lett. 26, 1221.

Lampe, M., Manheimer, W.M., McBride, J.B., Orens, J.H., Papadopoulos, K., Shanny, R., and Sudan, R.N.: 1972, Phys. Fluids 15, 662.

Lampe, M., Manheimer, W., and Papadopoulos, K.: 1975, NRL Memo Rept. 3076, ADA-014-411.

Lee, L.C.: 1982, Geophys. Res. Lett. 9, 1159.

Papadopoulos, K., Davidson, R.C., Dawson, J.M., Haber, I., Hammer, D.A., Krall, N.A., and Shanny, R.: 1971, Phys. Fluids 14, 849.

Papadopoulos, K.: 1979, Dynamics of the Magnetosphere, Ed. Akasofu, S.-I., D. Reidel, 289.

Sanderson, J.J., and Priest, E.R.: 1972, *Plasma Phys.* 14, 959.

Sato, T., and Hyashi, T.: 1979, *Phys. Fluids* 22, 1189.

Sato, T.: 1983, *these proceedings*.

Stenzel, R.L., Gekelman, W., and Wild, N.: 1982, *J. Geophys. Res.* 87, 111.

Tanaka, M., and Sato, T.: 1981, *J. Geophys. Res.* 86, 5541.

Ugai, M.: 1983, *Phys. Fluids* 26, 1569.

Vasyliunas, V.M.: 1975, *Rev. Geophys. Space Phys.* 13, 303.

Winske, D.: 1979, *Phys. Fluids* 24, 1069.

Wong, H.V.: 1970, *Phys. Fluids* 13, 757.

DISTRIBUTION LIST

PLEASE DISTRIBUTE ONE COPY TO EACH OF THE FOLLOWING PEOPLE (UNLESS OTHERWISE NOTED)

NAVAL RESEARCH LABORATORY
WASHINGTON, D.C. 20375
Dr. P. MANGE - CODE 4101
Dr. P. GOODMAN - CODE 4180

A.F. GEOPHYSICS LABORATORY
L.G. HANSCOM FIELD
BEDFORD, MA 01730
DR. T. ELKINS
DR. W. SWIDER
MRS. R. SAGALYN
DR. J.M. FORBES
DR. T.J. KENESHEA
DR. W. BURKE
DR. H. CARLSON
DR. J. JASPERSE

BOSTON UNIVERSITY
DEPARTMENT OF ASTRONOMY
BOSTON, MA 02215
DR. J. AARONS

CORNELL UNIVERSITY
ITHACA, NY 14850
DR. W.E. SWARTZ
DR. D. FARLEY
DR. M. KELLEY

HARVARD UNIVERSITY
HARVARD SQUARE
CAMBRIDGE, MA 02138
DR. M.B. McELROY
DR. R. LINDZEN

INSTITUTE FOR DEFENSE ANALYSIS
400 ARMY/NAVY DRIVE
ARLINGTON, VA 22202
DR. E. BAUER

MASSACHUSETTS INSTITUTE OF
TECHNOLOGY
PLASMA FUSION CENTER
LIBRARY, NW16-262
CAMBRIDGE, MA 02139

NASA
GODDARD SPACE FLIGHT CENTER
GREENBELT, MD 20771
DR. K. MAEDA
DR. S. CURTIS
DR. M. DUBIN
DR. N. MAYNARD - CODE 696

COMMANDER
NAVAL AIR SYSTEMS COMMAND
DEPARTMENT OF THE NAVY
WASHINGTON, D.C. 20360
DR. T. CZUBA

COMMANDER
NAVAL OCEAN SYSTEMS CENTER
SAN DIEGO, CA 92152
MR. R. ROSE - CODE 5321

NOAA
DIRECTOR OF SPACE AND
ENVIRONMENTAL LABORATORY
BOULDER, CO 80302
DR. A. GLENN JEAN
DR. G.W. ADAMS
DR. D.N. ANDERSON
DR. K. DAVIES
DR. R.F. DONNELLY

OFFICE OF NAVAL RESEARCH
800 NORTH QUINCY STREET
ARLINGTON, VA 22217
DR. G. JOINER

PENNSYLVANIA STATE UNIVERSITY
UNIVERSITY PARK, PA 16802
DR. J.S. NISBET
DR. P.R. ROHRBAUGH
DR. L.A. CARPENTER
DR. M. LEE
DR. R. DIVANY
DR. P. BENNETT
DR. F. KLEVANS

SCIENCE APPLICATIONS, INC.
1150 PROSPECT PLAZA
LA JOLLA, CA 92037
DR. D.A. HAMLIN
DR. E. FRIEMAN

STANFORD UNIVERSITY
STANFORD, CA 94305
DR. P.M. BANKS

U.S. ARMY ABERDEEN RESEARCH
AND DEVELOPMENT CENTER
BALLISTIC RESEARCH LABORATORY
ABERDEEN, MD
DR. J. HEIMERL

GEOPHYSICAL INSTITUTE
UNIVERSITY OF ALASKA
FAIRBANKS, AK 99701
DR. L.E. LEE

UNIVERSITY OF CALIFORNIA,
BERKELEY
BERKELEY, CA 94720
DR. M. HUDSON

UNIVERSITY OF CALIFORNIA
LOS ALAMOS SCIENTIFIC LABORATORY
J-10, MS-664
LOS ALAMOS, NM 87545
DR. M. PONGRATZ
DR. D. SIMONS
DR. G. BARASCH
DR. L. DUNCAN
DR. P. BERNHARDT
DR. S.P. GARY

UNIVERSITY OF MARYLAND
COLLEGE PARK, MD 20740
DR. K. PAPADOPOULOS
DR. E. OTT

JOHNS HOPKINS UNIVERSITY
APPLIED PHYSICS LABORATORY
JOHNS HOPKINS ROAD
LAUREL, MD 20810
DR. R. GREENWALD
DR. C. MENG

UNIVERSITY OF PITTSBURGH
PITTSBURGH, PA 15213
DR. N. ZABUSKY
DR. M. BIONDI
DR. E. OVERMAN

UNIVERSITY OF TEXAS
AT DALLAS
CENTER FOR RESEARCH SCIENCES
P.O. BOX 688
RICHARDSON, TX 75080
DR. R. HEELIS
DR. W. HANSON
DR. J.P. McCLURE

UTAH STATE UNIVERSITY
4TH AND 8TH STREETS
LOGAN, UTAH 84322
DR. R. HARRIS
DR. K. BAKER
DR. R. SCHUNK
DR. J. ST.-MAURICE

PHYSICAL RESEARCH LABORATORY
PLASMA PHYSICS PROGRAMME
AHMEDABAD 380 009
INDIA
P.J. PATHAK, LIBRARIAN

Director
Naval Research Laboratory
Washington, D.C. 20375

ATTN: Code 4700 (26 Copies)
Code 4701
Code 4780 (100 copies)
Code 4187 (E. Szuszczewicz)
Code 4187 (P. Rodriguez)
Code 2628 (22 copies)

University of Alaska
Geophysical Institute
Fairbanks, Alaska 99701

ATTN: Library
S. Akasofu
J. Kan
J. Roederer
L. Lee

University of Arizona
Dept. of Planetary Sciences
Tucson, Arizona 85721
ATTN: J.R. Jokipii

University of California, S.D.
LaJolla, California 92037
(Physics Dept.):

ATTN: J.A. Fejer
T. O'Neil
J. Winfrey
Library
J. Malmberg

(Dept. of Applied Sciences):
ATTN: H. Booker

University of California
Los Angeles, California 90024
(Physic Dept.):

ATTN: J.M. Dawson
B. Fried
J.G. Morales
W. Gekelman
R. Stenzel
Y. Lee
A. Wong
F. Chen
M. Ashour-Abdalla
Library
J.M. Cornwall

(Institute of Geophysics and
Planetary Physics):

ATTN: Library
C. Kennel
F. Coroniti

Columbia University
New York, New York 10027

ATTN: R. Taussig
R.A. Gross

University of California
Berkeley, California 94720
(Space Sciences Laboratory):

ATTN: Library
M. Hudson

(Physics Dept.):

ATTN: Library
A. Kaufman
C. McKee

(Electrical Engineering Dept.):
ATTN: C.K. Birdsall

University of California
Physics Department
Irvine, California 92664

ATTN: Library
G. Benford
N. Rostoker
C. Robertson
N. Rynn

California Institute of Technology
Pasadena, California 91109

ATTN: R. Gould
L. Davis, Jr.
P. Coleman

University of Chicago
Enrico Fermi Institute
Chicago, Illinois 60637

ATTN: E.N. Parker
I. Lerche
Library

University of Colorado
Dept. of Astro-Geophysics
Boulder, Colorado 80302
ATTN: M. Goldman
Library

Cornell University
School of Applied and Engineering Physics
College of Engineering
Ithaca, New York 14853
ATTN: Library
R. Sudan
B. Kusse
H. Fleischmann
C. Wharton
F. Morse
R. Lovelace

Harvard University
Cambridge, Massachusetts 02138
ATTN: Harvard College Observatory
(Library)
G.S. Vaina
M. Rosenberg

Harvard University
Center for Astrophysics
60 Garden Street
Cambridge, Massachusetts 02138
ATTN: G.B. Field

University of Iowa
Iowa City, Iowa 52240
ATTN: C.K. Goertz
D. Gurnett
G. Knorr
D. Nicholson

University of Houston
Houston, Texas 77004
ATTN: Library

University of Maryland
Physics Dept.
College Park, Maryland 20742
ATTN: K. Papadopoulos
H. Rowland
C. Wu

University of Michigan
Ann Arbor, Michigan 48140
ATTN: E. Fontheim

University of Minnesota
School of Physics
Minneapolis, Minnesota 55455
ATTN: Library
J.R. Winckler
P. Kellogg

M.I.T.
Cambridge, Massachusetts 02139
ATTN: Library
(Physics Dept.):
ATTN: B. Coppi
V. George
G. Bekefi
T. Dupree
R. Davidson
(Elect. Engineering Dept.):
ATTN: R. Parker
A. Bers
L. Smullin
(R.L.E.):
ATTN: Library
(Space Science):
ATTN: Reading Room

Princeton University
Princeton, New Jersey 08540
Attn: Physics Library
Plasma Physics Lab. Library
C. Oberman
F. Perkins
T.K. Chu
H. Okuda
V. Aranasalan
H. Hendel
R. White
R. Kulsrud
H. Furth
S. Yoshikawa
P. Rutherford

Rice University
Houston, Texas 77001
Attn: Space Science Library
R. Wolf

University of Rochester
Rochester, New York 14627
ATTN: A. Simon

Stanford University
Institute for Plasma Research
Stanford, California 94305
ATTN: Library

Stevens Institute of Technology
Hoboken, New Jersey 07030
ATTN: B. Rosen
G. Schmidt
M. Seidl

University of Texas
Austin, Texas 78712
ATTN: W. Drummond
V. Wong
D. Ross
W. Horton
D. Choi
R. Richardson
G. Leifeste

College of William and Mary
Williamsburg, Virginia 23185
Attn: F. Crownfield

Lawrence Livermore Laboratory
University of California
Livermore, California 94551
ATTN: Library
B. Kruer
J. Thomson
J. Nucholls
J. DeGroot
L. Wood
J. Emmett
B. Lasinsky
B. Langdon
R. Briggs
D. Pearlstein

Los Alamos National Laboratory
P.O. Box 1663
Los Alamos, New Mexico 87545
ATTN: Library
D. Forslund
J. Kindel
B. Bezzerides
H. Dreicer
J. Ingraham
R. Boyer
C. Nielson
E. Lindman
L. Thode

N.O.A.A.
325 Broadway S.
Boulder, Colorado 80302
ATTN: J. Weinstock
Thomas Moore (SEL, R-43)
W. Bernstein
D. Williams

Sandia Laboratories
Albuquerque, New Mexico 87115
ATTN: A. Toepfer
G. Yeonas
D. VanDevender
J. Freeman
T. Wright

Bell Laboratories
Murray Hill, New Jersey 07974
ATTN: A. Hasegawa

Lockheed Research Laboratory
Palo Alto, California 94304
ATTN: M. Walt
J. Cladis

Physics International Co.
2400 Merced Street
San Leandro, California 94577
ATTN: J. Benford
S. Putnam
S. Stalings
T. Young

Science Applications, Inc.
Lab. of Applied Plasma Studies
P.O. Box 2351
LaJolla, California 92037
ATTN: L. Linson
J. McBride

Goddard Space Flight Center
Greenbelt, Maryland 20771
ATTN: M. Goldstein
T. Northrop
T. Birmingham

TRW Space and Technology Group
Space Science Dept.
Building R-1, Room 1170
One Space Park
Redondo Beach, California 90278
ATTN: R. Fredericks
W.L. Taylor

National Science Foundation
Atmospheric Research Section (ST)
Washington, D.C. 20550
ATTN: D. Peacock

Goddard Space Flight Center
Code 620
Greenbelt, Maryland 20771
ATTN: Robert F. Benson

NASA Headquarters
Code EE-8
Washington, D.C. 20546
ATTN: Dr. I. Schmerling
Dr. J. Lynch
Dr. D. Butler

Klumper, David
Center for Space Sciences
P.O. Box 688
University of Texas
Richardson, Texas 75080

Leung, Philip
Dept. of Physics
University of California
405 Hilgard Avenue
Los Angeles, California 90024

Lysak, Robert
School of Physics and Astronomy
University of Minnesota
Minneapolis, MN 55455

Schulz, Michael
Aerospace Corp.
A6/2451, P.O. Box 92957
Los Angeles, California 90009

Shawhan, Stanley
Dept. of Physics & Astronomy
University of Iowa
Iowa City, Iowa 52242

Temerin, Michael
Space Science Lab.
University of California
Berkeley, California 94720

Vlahos, Loukas
Dept. of Physics
University of Maryland
College Park, Maryland 20742

Matthews, David
IPST
University of Maryland
College Park, Maryland 20742

Schunk, Robert W.
Utah State University
Dept. of Physics
Logan, Utah 84322

END

FILMED

1-84

DTIC